行政院國家科學委員會補助專題研究計畫成果報告

※※※※※※※※※※※※※※※※※※※※※※※※※
※　　　　　　　　　　　　　　　　　　　　　　　　※
※　　介電材料多層薄膜中微觀熱傳現象研究(2/2)　　※
※　　　　　　　　　　　　　　　　　　　　　　　　※
※※※※※※※※※※※※※※※※※※※※※※※※※

計畫類別：☑個別型計畫　　□整合型計畫

計畫編號：NSC　90－2212－E－009－073

執行期間：90 年 08 月 01 日至 91 年 07 月 31 日

計畫主持人：曲新生

本成果報告包括以下應繳交之附件：

□赴國外出差或研習心得報告一份

□赴大陸地區出差或研習心得報告一份

□出席國際學術會議心得報告及發表之論文各一份

□國際合作研究計畫國外研究報告書一份

執行單位：國立交通大學機械工程學系

中　華　民　國　91 年　10 月　14 日

行政院國家科學委員會專題研究計畫成果報告

介電材料多層薄膜中微觀熱傳現象研究(2/2)

Microscale Heat Transfer in Dielectric Multi-layer Thin Films (II)

計畫編號：NSC 90-2212-E-009-073

執行期限：90 年 08 月 01 日至 91 年 07 月 31 日

主持人：曲新生　　國立交通大學機械系

中文摘要

本研究從微觀的觀點來探討介電材料薄膜內的暫態熱傳現象。利用聲子輻射熱傳模式分析鑽石及砷化鎵/砷化鋁超晶格薄膜的熱傳行為。以散異模式(DMM)模擬薄膜與基材間或薄膜與薄膜間的熱阻。找出薄膜尺寸及幾何形狀對微系統等效熱傳導係數的影響。

關鍵詞：暫態熱傳、介電材料薄膜、微觀熱傳、等效熱傳導係數

ABSTRACT

This research studies transient heat transfer phenomena in solid dielectric thin films from microscopic point of view. Phonon radiative transfer model is utilized to analyze the transient heat conduction phenomena in dielectric thin films. Diamond and GaAs thin films are chosen as the example to demonstrate the differences between the macroscale and microscale heat transfer models. Diffuse Mismatch Model is chosen to simulate the interface condition. The purpose of this study is to find out the influences of size and geometry on the effective thermal conductivity of thin films.

Keywords: transient heat transfer, dielectric thin films, microscale heat transfer, effective thermal conductivity

1. INTRODUCTION

Microscale heat conduction has attracted great attention in the past due to the reduction of device sizes to the micrometer and nanometer range. The reduction of device sizes increased the device switching speed, and then enlarged the amount of heat generation [1]. Since the temperature of solid-state devices has significant influence on their performance, how to dissipate the heat becomes a vital issue. Experimental results of thermal conductivity measurements demonstrate that the thermal conductivities of thin films are often smaller than those of their corresponding bulk materials [2-4]. This implies that the Fourier law is inappropriate to treat microscale heat transfer in solids.

Heat transfer in solids is conducted by electrons and lattice vibrations. In metals, the contribution of electrons is dominant, whereas in dielectrics and semiconductors, vibrations of crystal lattice donate a majority of heat conduction. The energy of lattice vibrations is quantized and the quantum of lattice vibrations is called a phonon [5]. The Boltzmann Transport Equation (BTE) is the most appropriate theory for describing phonon transport in solids because it is able to correctly describe both equilibrium and non-equilibrium phenomena [6]. Based on the BTE, Majumdar [7] developed an equation of phonon radiative transfer (EPRT) to deal with microscale heat conduction in dielectric thin films. Joshi & Majumdar [8] employed the numerical scheme to simulate the transient behavior of heat in dielectric thin films. Chen et al. [9] analyzed the thermal conductivities of quantum well structures by solving the EPRT. The results showed that the thermal conductivities of the quantum well reduced one order of magnitude than that of its corresponding bulk material at room temperature. Furthermore, Chen [10] extended the applicability of EPRT to nanoparticles. The different between BTE and Fourier's law is ascribed to the nonlocal and nonquilibrium nature of the involved transport processes.

In practical engineering applications, thin films are almost always on supporting substrates and/or in multilayer configurations. In addition to size effect, the interface plays an important role in determining heat flow in thin-film/substrate systems. For example, a restriction in heat flow from the superconducting film can cause a transition from the superconducting state to the normal state during operation of the device, resulting in device failure. Some experiments [11,12] have been conducted to determine the interface thermal resistance between thin films and substrates. Besides the experimental quantification of interface thermal resistance, theoretical analysis also has been done by many researchers. Little [13] predicted interface thermal resistance by treating phonons as plane waves and proposed the acoustic mismatch model (AMM). An essential assumption of the AMM is that no scattering occurs at the interface. Swartz and Pohl [14] considered the diffuse scattering occurring at the interface and proposed the diffuse mismatch model (DMM). Phelan [15] pointed out that the AMM and DMM applicability is determined by the ratio $a_d/\pm$, where a_d is the dominant phonon wavelength, and $\pm$ is the mean interfacial roughness. When $a_d/\pm >> 1$, the AMM is applicable, otherwise,

the DMM applies. Chen [16] examined the effect of interface conditions on the thermal conductivity of superlattices. The DMM results were in reasonable agreement with experimental results of Capinski and Maris on a GaAs/AlAs superlattices [17].

The purpose of this study is to find out the influences of size and geometry on the effective thermal conductivity of thin films. First, the size effects (thickness and height) and curvature effects on the effective thermal conductivity for two-dimensional micro tubes are studied. Then, the microscale heat transfer for a two-layer concentric circular tube with interface thermal resistance are also examined. Finally, the results are compared to the experimental data.

2. ANALYSIS

Phonon heat transfer in dielectric thin films can be modeled by the Boltzmann transport equation [7]. Under the first-order relaxation time approximation, the BTE is reduced to

$$\frac{\partial f_\mu}{\partial t} + \vec{v}\cdot\nabla f_\mu = \frac{f_\mu^0 - f_\mu}{\tau_R}. \quad (1)$$

Where f_μ is the phonon distribution function as a function of frequency μ, f_μ^0 is the equilibrium distribution function, $\vec{v} = v\vec{e}_v$ is the group velocity, and τ_R is the relaxation time. The intensity of phonons can be represented as follows

$$I_\mu = \sum_p v f_\mu \hbar\mu D(\mu). \quad (2)$$

$\hbar$ is the Planck's constant divided by 2π, D is the density of states, and the summation index p is the phonon polarization. Substituting Eq. (2) into Eq. (1), Majumdar [7] transformed the BTE to

$$\frac{1}{v}\frac{\partial I_\mu}{\partial t} + \vec{e}_v\cdot\nabla I_\mu = \frac{I_\mu^0 - I_\mu}{\tau_R v}. \quad (3)$$

For a one-dimensional two-layer concentric circular tube, the governing equations can be derived as

$$\frac{1}{v_k}\frac{\partial I_k}{\partial t} + \mu\frac{\partial I_k}{\partial r} - \frac{1}{r}\eta\frac{\partial I_k}{\partial\omega} = \frac{\frac{1}{4\pi}\int_{t=4\pi} I_k\,d\Omega - I_k}{\tau_R v_k}, \quad k = 1, 2 \quad (4)$$

The subscript $k = 1$ and 2 represent layer 1(inner layer) and layer 2(outer layer), respectively.

For a two-dimensional micro tube, Eq.(3) is transformed to

$$\frac{1}{v}\frac{\partial I}{\partial t} + \frac{\mu}{r}\left[\frac{\partial(rI)}{\partial r}\right] - \frac{1}{r}\left[\frac{\partial(\eta I)}{\partial\omega}\right] + \xi\left[\frac{\partial I}{\partial z}\right] = \frac{\frac{1}{4\pi}\int_{4\pi} I\,d\Omega - I}{v\tau_R}. \quad (5)$$

The constant temperature boundary condition is

$$I(B) = I^0(T_B), \quad (6)$$

where B means the boundary. Energy balance at the interface $(r = r_b)$ between layer 1 and layer 2 gives [16]

$$\int_{2\pi} I_i^-(r_b, -\mu_i)\mu_i d\mu_i = R_{ij}\int_{2\pi} I_i^+(r_b, \mu_i)\mu_i d\mu_i + \tau_{ji}\int_{2\pi} I_j^-(r_b, -\mu_j)\mu_j d\mu_j, \quad i, j = 1, 2. \quad (7)$$

Where R_{ij} and τ_{ij} represent the energy reflectivity and transmissivity at the interface for phonons incident from layer i towards layer j.

3. METHOD OF SOLUTION

The discrete ordinate method is utilized to solve the governing equation. The integral term in the governing equation is approximated by Gaussian quadrature

$$\int_{t=4\pi} I\,d\Omega = \sum_{i=1}^{m} I_i w_i, \quad (8)$$

where w_i are the weighting factors.

After discretizing the governing equation, we get a set of simultaneous equations. Thus a iterative method is used to solve this problem. The convergence criterion is that the relative error is less than 10^{-4}.

4. RESULTS AND DISCUSSION

CASE(I):

Fig. 1 is the physical model of a two-layer concentric circular tube. It is known that Fourier law is inadequate to analyze microscale heat transfer behavior. However, the concept of effective thermal conductivity is an efficient way to calculate the heat transfer rate. In order to show the effect of film thickness on the thermal conductivity, the plane-parallel GaAs/AlAs superlattices are chosen as the demonstration. Fig. 2 reveals that the thermal conductivity of GaAs/AlAs superlattices is smaller than its bulk value. In addition, the thermal conductivity decreases as film thickness decreases. The simulation results agree with the experimental data very well. Thus, the miniaturization of microelectronic devices will reduce the ability of heat transfer and causes the failure of devices if the size effect is ignored.

Fig. 3 illustrates the effect of curvature on the thermal conductivity of GaAs/AlAs superlattices. Three inner radii: $r_i = 10^{-5}$, $r_i = 10^{-6}$, and $r_i = 10^{-7}$ are chosen as examples. It can be seen that the thermal conductivity increases with the increase of curvature. This phenomenon is amplified by large tube thickness. However, there is no obvious difference among these three cases when the tube is getting thin. The effect of curvature on thermal conductivity becomes less important. Size effect rather than curvature effect dominates the heat transfer behavior in an ultra-thin tube.

CASE(II):

Fig. 4 is the physical model of a two-dimensional micro tube. Fig. 5 shows the size effects on the thermal conductivity under different tube heights in the radial and axial directions. The thermal conductivity of diamond micro tubes is smaller than its bulk value. The radial thermal conductivity decreases as tube thickness decreases. Similarly, the radial thermal conductivity of a tube with $L_a = 1\,\mu$ is small than that of $L_a = 50\,\mu$. It can be concluded that the reduction of size, no matter the radial or axial directions, will reduce the thermal conductivity of the material. From Fig. 5(a), it is noticed that the radial thermal conductivity approaches to the bulk value when the tube is getting thick. Fig. 5 (b) have similar trend as Fig. 5(a). However, the axial thermal conductivity varies very small as the tube thickness decreases. The tube height is more important than the tube thickness in calculating the axial thermal conductivity. The axial thermal conductivity does not approach the bulk value if the tube is short. The small tube height restricts the axial thermal conductivity growing although the tube is thick enough.

Fig. 6 depicts the effect of curvature on the radial and axial thermal conductivity at different tube heights. The radial and axial thermal conductivities do not vary with different curvature. The effect of tube curvature is not significant to the effective thermal conductivity.

5. CONCLUSIONS

EPRT is employed to model the microscale heat conduction within thin tubes. DMM is utilized to describe the interface condition between two dissimilar layers. And then the discrete ordinate method is used for numerical analysis. The results sow that the reduction of size (thickness and height) will reduce the effective thermal conductivity. In addition, the effective thermal conductivity increases as the curvature increases. However, the size and curvature effects on interface thermal resistance are not significant when the DMM is employed to describe the interface condition.

6. REFERENCES

1. Tien, C. L., Majumdar, A., and Gerner, F. M., Microscale Energy Transport, Taylor & Francis, Washington, DC, 1998.
2. Lambropoulos, J. C., Jacobs, S. D., Burns, S. J., Shaw-Klein, L., and Hwang, S. S., Thermal Conductivity of Thin Films: Measurement and Microstructural Effects, ASME HTD, Vol. 184, pp. 21-32, 1991.
3. Tien, C. L. and Chen, G., Challenges in Microscale Radiative and Conductive Heat Transfer, ASME J. Heat Transfer, Vol. 116, pp. 799-807, 1994.
4. Lee, S. M. and Cahill, D. G., Heat Transport in Thin Dielectric Films, J. Appl. Phys., Vol. 81, pp. 2590-2595, 1997.
5. Kittel, C., Introduction to Solid State Physics, 6th ed., John Wiley and Sons, New York, 1986.
6. Mazumder, S. and Majumdar, A., Monte Carlo Study of Phonon Transport in Solids in Thin Films Including Dispersion and Polarization, ASME J. Heat Transfer, Vol. 123, pp. 749-759, 2001.
7. Majumdar, A., Microscale Heat Conduction in Dielectric Thin Films, ASME J. Heat Transfer, Vol. 115, pp. 7-16, 1993.
8. Joshi, A. A. and Majumdar, A., Transient Ballistic and Diffusive Phonon Heat Transport in Thin Films, J. Appl. Phys., Vol. 74, pp. 31-39, 1993.
9. Chen, G. and Tien, C. L., Thermal Conductivities of Quantum Well Structure, J. Thermophysics and Heat Transfer, Vol. 7, pp. 311-318, 1993.
10. Chen, G., Nonlocal and Nonequilibrium Heat Conduction in the Vicinity of Nanoparticles, ASME J. Heat Transfer, Vol. 118, pp. 539-345, 1996.
11. Nahum, M., Verghese, S., Richards, P. L., and Char, K., Thermal Boundary Resistance for $YBa_2Cu_3O_{7-\delta}$ Films, Applied Physics Letters, Vol. 59, pp. 2034-2036, 1991.
12. Kelkar, M., Phelan, P. E., and Gu, B., Thermal Boundary Resistance for Thin-Film High-T_c Superconductors at Varying Interfacial Temperature Drops, Int. J. Heat Mass Transfer, Vol. 40, pp. 2637-2645, 1997.
13. Little, W. A., The Transport of Heat between Dissimilar Solid at Low Temperature, Can. J. Phys., Vol. 37, pp. 334-349, 1959.
14. Swartz, E. T. and Pohl, R. O., Thermal Boundary Resistance," Reviews of Modern Physics, Vol. 61, pp. 605-668, 1989.
15. Phelan, P. E., Application of Diffuse Mismatch Theory to the Prediction of Thermal Boundary Resistance in Thin-Film High-T_c Superconductors, ASME J. Heat Transfer, Vol. 120, pp. 37-43, 1998.
16. Chen, G., Thermal Conductivity and Ballistic-Phonon Transport in the Cross-Plane Direction of Superlattices, Physical Review B, Vol. 57, pp. 14958-14973, 1998.
17. Capinski, W. S. and Maris, H. J., Thermal Conductivity of GaAs/AlAs Superlattices, Physica B, Vol. 220, pp. 699-701, 1996.

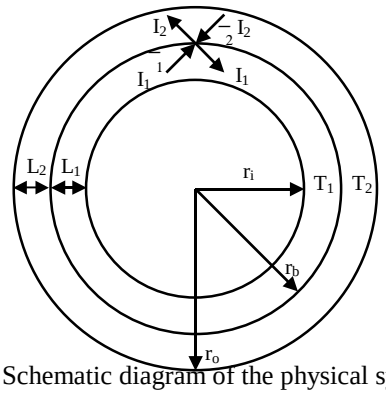

Fig. 1 Schematic diagram of the physical system.

Fig. 2 Effect of film thickness on the thermal conductivity of GaAs/AlAs superlattices.

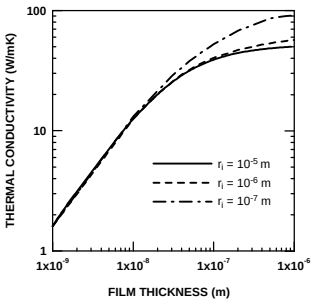

Fig. 3 Effect of curvature on the thermal conductivity of GaAs/AlAs superlattices.

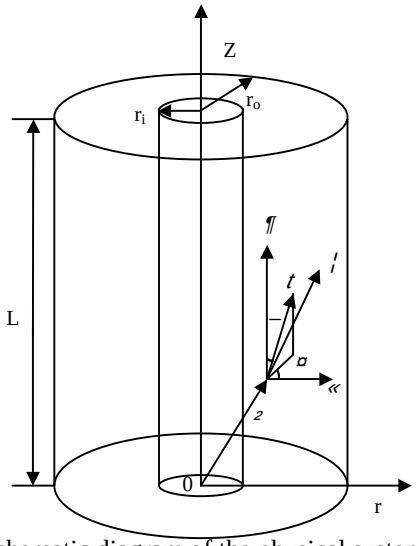

Fig. 4 Schematic diagram of the physical system.

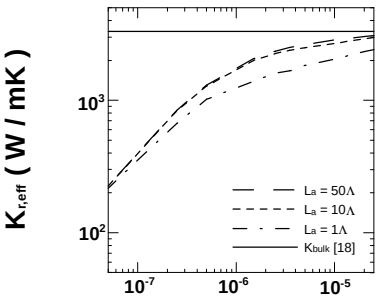

Fig. 5(a) Size effects on the radial thermal conductivity under different tube heights.

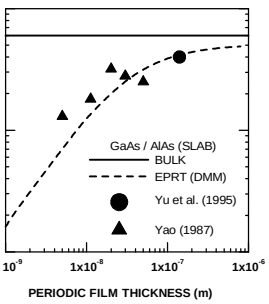

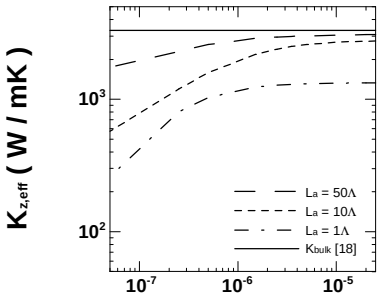

Fig. 5(b) Size effects on the axial thermal conductivity under different tube heights.

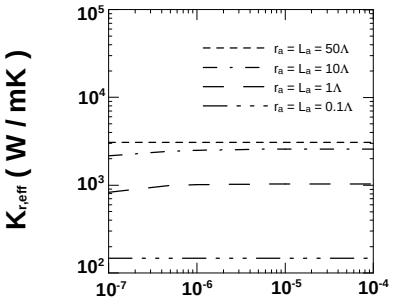

Fig. 6(a) The effect of curvature on the radial thermal conductivity for different tube heights.

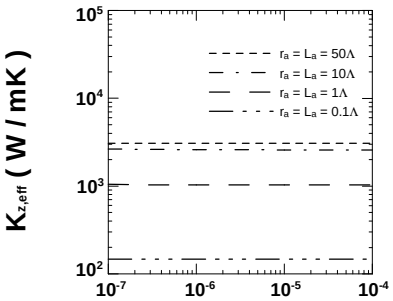

Fig. 6(b) The effect of curvature on the axial thermal conductivity for different tube heights.